Antiferromagnetic Coupling Driven by Bond Length Contraction near the Ga1-xMnxN Film Surface

Antiferromagnetic Coupling Driven by Bond Length Contraction near the $Ga_{1-x}Mn_xN$ Film Surface

Q. Wang, Q. Sun, and P. Jena*

Physics Department, Virginia Commonwealth University, Richmond, Virginia 23284-2000, USA

Y. Kawazoe

Institute for Material Research, Tohoku University, Sendai, 980-8577, Japan

Using first principles calculations based on gradient corrected density functional theory we show that Mn atoms, which couple ferromagnetically in bulk $Ga_{1-x}Mn_xN$, couple antiferromagnetically on its surface. This change in magnetic behavior is brought about by a contraction of the Mn-Mn and Mn-N bond lengths, which is significantly greater on the surface than in the bulk. The present study provides new insight to the numerous conflicting experimental observations in Mn doped GaN systems.

Spintronics, which exploits an electron's spin degree of freedom to store and carry information, has the potential to revolutionize the electronics industry. To this end the dilute magnetic semiconductors (DMS) are considered to be an important class of materials. Following the discovery of ferromagnetism in (Ga, Mn)As [1] and the subsequent theoretical prediction [2] that Mn doped GaN could be ferromagnetic at or above room temperature, numerous attempts have been made to synthesize this promising DMS material [3–19]. However, the results have been rather confusing. Not only do the reported Curie temperatures [3–14] vary over a wide range (10–945 K), but also it is uncertain whether the ground state of (Ga, Mn)N is ferromagnetic (FM) or antiferromagnetic (AFM) [15–21]. It has been found that at low temperature (< 10 K) the magnetic behavior of the (Ga, Mn)N layers prepared by reactive molecular beam epitaxy shows AFM characteristics with a spin-glass transition [17]. Magnetic measurement at $T = 2$ K using the superconducting quantum interference device magnetometer also shows AFM coupling between Mn ions in the (Ga, Mn)N sample [18]. An understanding of the controversy between FM and AFM is both important and challenging [20,21].

To understand the origin of magnetism in Mn doped GaN, several theoretical studies have recently been performed. However, all the reported calculations predicted ferromagnetism for $Ga_{1-x}Mn_xN$ [22–28], and no study has been reported to explain the AFM coupling observed in experiments. We should note that these theoretical calculations correspond to the bulk $Ga_{1-x}Mn_xN$ system, while the AFM ordering seen experimentally corresponds to thin films synthesized using molecular beam epitaxy and metal-organic chemical vapor deposition. In addition, previous theoretical studies used either the tight binding method or conventional pseudopotentials and did not fully relax the geometry following Mn substitu-

tion. In some studies, the AFM configurations were not even considered.

In this Letter, we have studied the magnetic properties of $Ga_{1-x}Mn_xN$ in both bulk and thin film forms by allowing full structural relaxation. Using density functional theory and generalized gradient approximation for exchange and correlation, we have calculated the total energies, electronic structure, and magnetic coupling for FM and AFM states in bulk and ($11\bar{2}0$) film having the wurtzite structure. Calculations have also been performed on the (110) film in the zinc blende structure, but these results will be published elsewhere. We show that bulk $Ga_{1-x}Mn_xN$ is FM with or without structural relaxation. On the contrary, the unrelaxed thin film is FM which becomes AFM after relaxation.

Calculations of the total energies and forces, and optimizations of geometry, were carried out using a plane-wave basis set with the projector augmented plane-wave (PAW) method [29] as implemented in the Vienna *ab initio* simulation package (VASP) [30]. The particular advantage of the PAW method over the conventional pseudopotentials and ultrasoft pseudopotentials is that it can improve the accuracy especially for magnetic systems and for materials including early d-electron or f-electron elements. The energy cutoff was set to 330 eV, and the convergence in energy and force were 10^{-4} eV and 3×10^{-3} eV/Å, respectively.

We begin the calculations with a bulk wurtzite structure. Using a supercell of $Ga_{14}Mn_2N_{16}$ with the experimental lattice constants ($a = b = 3.189$, $c = 5.185$ Å) and the ($6 \times 6 \times 6$) Monkhorst-Pack [31] k-point mesh, and putting the two Mn atoms along the [$10\bar{1}0$] direction linked by a N atom, we found that without the structure optimization the coupling between these two Mn atoms is FM as predicted by previous studies [22–28]. The FM state lies 0.053 eV lower in energy than the AFM state.

When the structure is fully relaxed without symmetry constraint, the Mn-N bond length is found to be 1.99 Å, which is in good agreement with the experimental value of 2.01 ± 0.03 Å [32]. The ground state of the system remained FM, although the energy difference between the AFM and the FM states is 0.077 eV. Therefore, the structure optimization in bulk did not change the FM coupling characteristic. This is due to the fact that the changes in structure for substitutional doping of Mn are minor in bulk.

We now discuss our results on thin film. We have modeled the thin film having $(11\bar{2}0)$ orientation and wurtzite structure by a slab of nine layers. The corresponding supercell contains 72 atoms (36 Ga and 36 N atoms). To preserve symmetry, the top and bottom layers of the slab were taken to be identical, and each slab was separated from the other by a vacuum region of 10 Å. The central three layers were held fixed at their bulk configuration while the three surface layers on either side of the slab were allowed to relax without any symmetry constraint. k-point convergence was achieved with the $(6 \times 4 \times 1)$ grid, and tests with up to $(8 \times 6 \times 2)$ mesh were made. Tests were also made on slabs containing 11 and 13 layers (88 and 104 atoms/supercell, respectively). We found that the slab with nine layers is adequate to mimic the thin film.

In Fig. 1 we show the supercell corresponding to the thin film. The darker numbered atoms are Ga, and the lighter atoms are N. To study the site preference of a *single*
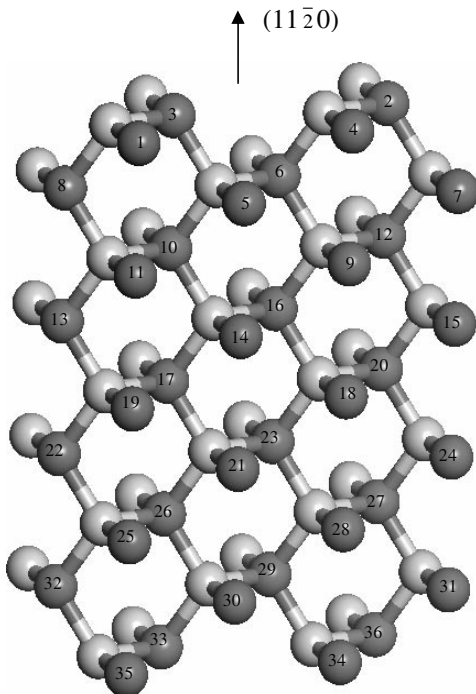

FIG. 1. The supercell of the $Ga_{1-x}Mn_xN$ $(11\bar{2}0)$ slab consisting of 36 Ga and 36 N atoms. The numbered atoms are Ga.

Mn atom, we replaced one Ga atom by Mn on the surface layer, the second layer, and the third layer and computed the total energies. Note that to preserve symmetry a corresponding Ga atom on the lower half of the slab was also replaced by Mn. We find that the Mn atom prefers to reside on the surface site which lies 1.37 and 1.54 eV below that of the second and the third layers, respectively. This is consistent with experiment where Mn atoms doped in GaN migrated to the surface site upon annealing [33].

To study the magnetic coupling between Mn atoms, it is necessary to replace at least two Ga atoms in the top half of the supercell by two Mn atoms. To preserve symmetry corresponding Ga atoms from the lower half of the slab were also replaced by Mn atoms. This amounts to a supercell consisting of $Ga_{32}Mn_4N_{36}$ (11% Mn concentration). There are many ways in which this substitution can be achieved. We have considered five different configurations. In Table I, we show which of the Ga atoms in Fig. 1 were replaced by Mn atoms for each of the five configurations. The relative energies of the FM and AFM states for each of the configuration are listed in Table I. Note that the energies are measured with respect to the ground state, which we find to be AFM with Mn atoms residing at nearest neighbor positions around the N atom on the surface layer. The corresponding FM state lies 0.40 eV higher in energy. In configurations of II, III, and IV, the energy difference between FM and AFM is small, but these configurations are much higher in energy relative to configuration I.

The total densities of states (DOS) for an unrelaxed and a fully relaxed $Ga_{32}Mn_4N_{36}$ thin film are shown in Figs. 2(a) and 2(b), respectively. For the unrelaxed surface, the coupling is FM and the DOS shows half-metallic behavior similar to that in $(Ga, Mn)N$ bulk. When the surface is fully relaxed, the coupling becomes AFM and the spin up and spin down DOS are identical as the total moment of the system is zero. The magnetic moment at each of the Mn sites is found to be $3.0\mu_B$ with opposite spin orientation, which is reduced as compared to the unrelaxed situation $(3.80\mu_B)$. The main contribution to this moment comes from the Mn $3d$ electrons as can be seen from the partial DOS for one Mn atom in Fig. 2(c).

TABLE I. Relative energies E(FM) and E(AFM) of the $Ga_{1-x}Mn_xN$ $(11\bar{2}0)$ thin film. ΔE is the energy difference between the AFM and FM states. In the configuration column, the positions of Mn ions are specified, as shown in Fig. 1.

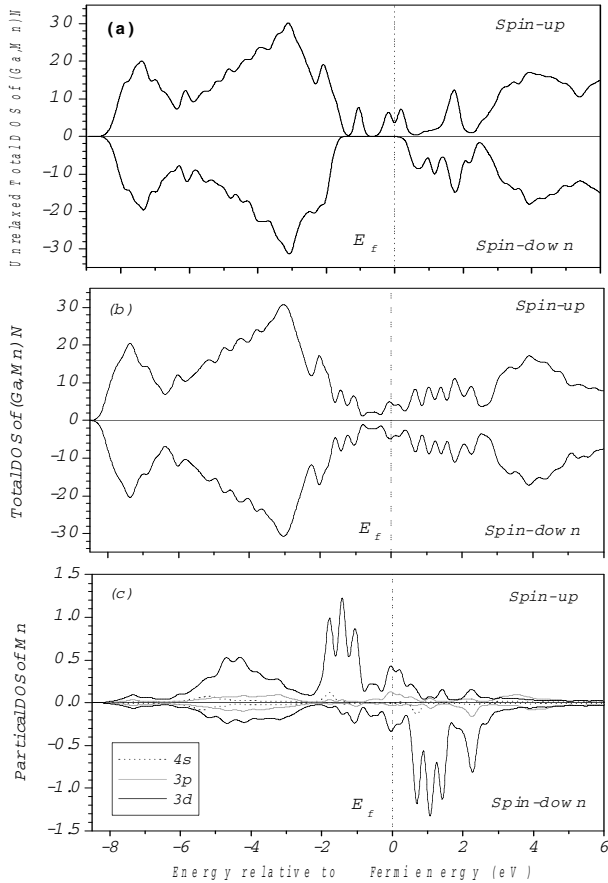| Configuration	E(FM)	E(AFM)	ΔE
I {1–3, 33–35}	+0.403	0.0	−0.403
II {2–3, 33–36}	+1.722	+1.694	−0.028
III {1–2, 35–36}	+1.773	+1.708	−0.065
IV {3–6, 29–33}	+2.550	+2.465	−0.085
V {5–6, 29–30}	+3.438	+3.226	−0.212

FIG. 2. Total DOS for (a) an unrelaxed (FM) and (b) a relaxed $Ga_{1-x}Mn_xN$ thin film in the AFM state. The corresponding partial DOS of the Mn atom are shown in (c).

The hybridization between N-$2p$ and Mn-$3d$ reduces the magnetic moment as compared to that of a free Mn atom.

As discussed above, the magnetic coupling between Mn atoms in the bulk is not affected by the relaxation of the structure. However, the situation is different for the surface case. If the surface is not relaxed, the coupling is FM, which becomes AFM upon optimization. To understand the physics involved, we checked the changes in bond lengths. Because of relaxation, the bond lengths near the film surface are contracted. For example, in the ground state the bond length of Mn-N (1.82 Å) and Mn-Mn (2.98 Å) in the first surface layer is significantly shorter than the corresponding bulk values (1.99 and 3.23 Å, respectively). It has been established that the magnetic couplings between Mn atoms are sensitive to the Mn-Mn distance [34–36]. For example, in ortho-rhombic and monoclinic-layered $LiMnO_2$, the coupling between two Mn atoms change from FM phase to AFM phase when the Mn-Mn distance changes from 2.82 to 2.79 Å [34]. In a recent report, Hobbs and his co-workers studied the distance dependence of the pairwise exchange interactions in a Heisenberg-like model for bulk Mn and found AFM coupling for short interatomic distances, which switches to FM coupling at larger distances. It is this sensitivity of magnetic coupling to the atomic distance that makes Mn-based materials display very complicated magnetic structures ranging from nonmagnetic to antiferromagnetic, low spin ferrimagnetic, and high spin ferromagnetic phases [35,36].

When going from the surface to the interior of the film, the bond length contraction vanishes gradually. Therefore, we can expect an evolution from antiferromagnetic to ferromagnetic coupling as one penetrates into subsurface layers. This is exactly what happens. Table II lists the changes in a magnetic state and a Mn-Mn bond length in going from the surface down to the inside of the bulk. Because in the ground state Mn atoms prefer to cluster around a N atom, we checked the possibility of such clustering for the first three layers. They correspond to the substituted Ga sites identified by $(1, 3)$, $(5, 6)$, and $(10, 11)$, respectively, on one side of the slab in Fig. 1. We found that the bond length contraction mainly occurs in the first two layers, and the magnetic couplings are AFM. In the third layer, the bond length is close to the bulk, and the coupling switches to being FM.

It is important to discuss the effect of supercell construction on the preferred magnetic coupling between Mn atoms in the bulk and the surface since the limited supercell sizes in both bulk and surface can allow the mirror images of Mn atoms from neighboring supercells to interfere. To clarify these points we have performed additional bulk and surface calculations with larger supercells. In the bulk $Ga_{14}Mn_2N_{16}$ supercell discussed above, the two Ga atoms on the (0001) plane were replaced by Mn. This gives rise to a continuous line of Mn atoms along the $[10\bar{1}0]$ direction separated by lines of Ga atoms. We therefore used a different $(3 \times 3 \times 2)$ supercell of $Ga_{34}Mn_2N_{36}$ to model the bulk case where the Ga atoms belonging to two adjacent (0001) planes linked by a N atom were replaced by Mn. In this way, no continuous Mn-atom line can be formed, and the minimum distance between Mn-N-Mn and its image is 8.0 Å. Using a $(5 \times 5 \times 5)$ Monkhorst-Pack grid we found the results to be nearly the same as that given earlier for the smaller supercell; namely, the ground state in the bulk is

TABLE II. Changes in magnetic state and bond length (Å) when going from the surface to the inside of bulk.

Layer	Coupling	R_{Mn-N}	R_{Mn-Mn}
1st	AFM	1.822	2.978
2nd	AFM	1.920	3.093
3rd	FM	1.951	3.111
Bulk	FM	1.990	3.233
		2.01 ± 0.03 (expt.)[a]	

[a]From Ref. [32].

FM and lies 0.10 eV lower in energy than the AFM state. The Mn-N bond length is 1.98 Å.

It is also legitimate to wonder if the regular distribution of Mn on the surface layer could also be responsible for the AFM coupling. For example, in the ground state configuration in Fig. 1 the Mn atoms form continuous chains along the [0001] direction. To examine if the AFM coupling in the surface could be due to this chain formation, we repeated the bulk calculations by using a $3 \times 3 \times 1$ supercell of $Ga_{16}Mn_2N_{18}$ where Mn atoms also form continuous chains in the bulk with the same [0001] orientation and the same 11% concentration as in the surface case. The minimum distance between the chain and its image in this bulk case is 8.44 Å. The calculation was performed with the $4 \times 4 \times 8$ k-point mesh. The ground state was found to be FM with the energy difference of 0.07 eV lower than the AFM state. We found the Mn-N and Mn-Mn bond lengths in the bulk chain are 1.98 and 3.10 Å, which are significantly larger than the corresponding values on the surface. Thus, the change in magnetic coupling when going from surface to bulk is associated with the change in bond length. We also performed calculations for a noncontinuous chain consisting of three Mn atoms along the [0001] direction on the surface by using a large $Ga_{50}Mn_6N_{56}$ supercell and the $4 \times 4 \times 2$ k-point mesh. The separation between the finite chain and its image in the [0001] direction is 5.2 Å. Again, the AFM state is found to be more stable than the FM state with the energy difference of 0.06 eV/Mn atom. The Mn-N bond length on the surface layer is 1.82 Å, and the Mn-Mn distance is 2.91 Å. Thus it is clear that the AFM coupling in the thin film is due to bond contraction.

From the standpoint of technological applications, doping of Mn beyond 1% is relatively easy only in the case of "soft" semiconductors like GaAs, InAs, or CdTe. This is not the case with "hard" semiconductors like GaN, which needs relatively high growth temperatures to obtain good crystalline quality. In order to obtain a high concentration of Mn, a highly nonequilibrium growth process is necessary. However, under those conditions Mn atoms in GaN will migrate to the surface layers upon annealing [33]. The bond length contraction in the surface layers would result in AFM coupling. Thus to maintain FM coupling between Mn atoms on the surface layer, their separation distance has to be increased by other means such as choosing the appropriate substrate for film growth or surface coating.

In summary, we have shown that in the (Ga, Mn)N system Mn-Mn separation distance plays a critical role in their magnetic coupling: The AFM coupling on or near the surface layers is driven by Mn-Mn bond length contraction. Thus if the sample growth conditions are such that Mn atoms are buried in the bulk, the coupling is FM.

However, if Mn atoms migrate to the surface, the coupling is AFM. Our results provide an understanding of the seemingly different experimental results.

*Corresponding author.
[1] H. Ohno, Science **281**, 951 (1998).
[2] T. Dietl *et al.*, Science **287**, 1019 (2000); H. Ohno *et al.*, Nature (London) **408**, 944 (2000).
[3] M. L. Reed *et al.*, Mater. Lett. **51**, 500 (2001).
[4] M. L. Reed *et al.*, Appl. Phys. Lett. **79**, 3473 (2001).
[5] S. Sonoda *et al.*, J. Cryst. Growth **237**, 1358 (2002).
[6] T. Sasaki *et al.*, J. Appl. Phys. **91**, 7911 (2002).
[7] G. T. Thaler *et al.*, Appl. Phys. Lett. **80**, 3964 (2002).
[8] J. M. Lee *et al.*, Microelectron. Eng. **69**, 283 (2003).
[9] P. P Chen *et al.*, J. Cryst. Growth **251**, 331 (2003).
[10] S. S. Seo *et al.*, Appl. Phys. Lett. **82**, 4749 (2003).
[11] Y. Shon *et al.*, J. Appl. Phys. **93**, 1546 (2003).
[12] T. Kondo *et al.*, J. Cryst. Growth **237**, 1353 (2002).
[13] M. E. Overberg *et al.*, Appl. Phys. Lett. **79**, 1312 (2001).
[14] K. Sardar *et al.*, Solid State Commun. **125**, 55 (2003).
[15] S. Dhar *et al.*, Appl. Phys. Lett. **82**, 2077 (2003).
[16] S. Dhar *et al.*, Phys. Rev. B **67**, 165205 (2003).
[17] K. H. Ploog *et al.*, J. Vac. Sci. Technol. B **21**, 1756 (2003).
[18] M. Zajac *et al.*, Appl. Phys. Lett. **79**, 2432 (2001).
[19] K. Ando, Appl. Phys. Lett. **82**, 100 (2003).
[20] T. Graf *et al.*, Phys. Status Solidi B **239**, 277 (2003).
[21] S. J. Pearton *et al.*, J. Phys. Condens. Matter **16**, R209 (2004).
[22] C. Y. Fong *et al.*, J. Electron. Mater. **29**, 1067 (2000).
[23] M. van Schilfgaarde and O. N. Mryasov, Phys. Rev. B **63**, 233205 (2003).
[24] K. Sato and H. K. Yoshida, Jpn. J. Appl. Phys. **40**, L485 (2001); Semicond. Sci. Technol. **17**, 367 (2002).
[25] L. Kronik *et al.*, Phys. Rev. B **66**, 041203 (2002).
[26] E. Kulatov *et al.*, Phys. Rev. B **66**, 045203 (2002).
[27] Yu. Uspenskii *et al.*, J. Magn. Magn. Mater. **258–259**, 248 (2003).
[28] G. P. Das *et al.*, Phys. Rev. B **68**, 035207 (2003).
[29] P. E. Blöchl, Phys. Rev. B **50**, 17 953 (1994).
[30] G. Kresse and J. Furthmüller, Phys. Rev. B **54**, 11 169 (1996).
[31] H. J. Monkhorst and J. D. Pack, Phys. Rev. B **13**, 5188 (1976).
[32] Y. L. Soo *et al.*, Appl. Phys. Lett. **79**, 3926 (2001).
[33] S. Prokes (private communication).
[34] G. Ceder and S. K. Mishra, Electrochem. Solid State Lett. **2**, 1 (1999).
[35] D. Hobbs, J. Hafner, and D. Spisak, Phys. Rev. B **68**, 014407 (2003).
[36] J. Hafner and D. Hobbs, Phys. Rev. B **68**, 014408 (2003).